

# Electrostriction Enhancement of Solid-State Capacitance Sensing

Yuri M. Shkel, *Associate Member, IEEE*, and Nicola J. Ferrier, *Member, IEEE*

**Abstract**—This paper analyzes the performance of a solid-state capacitance sensor that extends classical modeling to incorporate an electrostriction model of isotropic linear elastic dielectrics. A capacitance sensor which incorporates an elastic dielectric layer between the electrodes exhibits higher sensitivity and is more robust than its air-gap or vacuum-gap counterparts. Sensors with polyester and urethane polymer dielectric layers are tested for the response to normal loads and are compared with air-gap setups of same geometry. Experimental data suggest that the solid-state sensor has linear response in loads range up to six orders of magnitude and demonstrates a two to three times stronger output signal than air-gap designs. Potential for future development and application of solid capacitance sensors is discussed.

**Index Terms**—Capacitive sensors, electrostriction, pressure, solid-state capacitor, strain, stress, tactile.

## I. INTRODUCTION

CAPACITANCE measurements of deformation and displacements have wide applicability in numerous mechatronic devices for stress, strain, pressure, and tactile sensing. Tactile sensors are widely used in manipulation tasks, automatic grasping, and compliance control (see [10] for a review). With few exceptions [5], [17], [20], tactile sensor arrays are mounted against a rigid backing and covered with a thin rubber layer to provide friction. In a comparative study, Shimoga and Goldenberg [21] showed that gel-filled membrane fingertips (e.g., [5], [11]) showed overall best performance in terms of attenuation of impact forces, conformability, and strain dissipation. Such fingertip designs have typically employed various intermediate layers of materials including foam, rubber, or gel to transmit stress/pressure to a stand-alone and functionally separated sensing unit, e.g., an air-gap or vacuum-gap capacitor. Displacement or deformation of the electrodes of a capacitor sensor induce a change in its capacitance. With a rigid coupling between the sensor and the sensed object a capacitance sensor measures deformation or displacements. With an elastic coupling provided, for example, by a deformable electrode, a capacitance sensor is capable of resolving a force applied to its surface. Thus, a set of capacitance sensors distributed over some surface is capable of resolving a distribution of normal force (i.e. a normal stress distribution) on the surface. Many of the tactile sensors employ capacitance arrays [4], [10] of pressure-sensitive elements to provide information on the

location of the contact and the stress distribution induced by the contact. However, the manufacture of a vacuum-gap capacitor can be difficult (although batch fabrication techniques for micromachining silicon air-gap devices are now available) and the devices cannot withstand large loads (for example, state of the art commercial sensors designed for 3–30 psi can withstand overpressures of 20–200 psi, factors of about 6 [19]).

In this paper, we present a design and modeling of a solid-state sensor that incorporates an elastic dielectric material between electrodes. Such a design affords a dynamic response of the sensor determined by properties of the material rather than properties of the electrodes. The solid-state approach overcomes shortcomings of air-gap or vacuum-gap capacitors such as lack of robustness, fragility, rigid backing, and cost, but retains the benefits of a capacitor sensing solution. In addition, the *electrostriction properties* of the dielectric material between electrodes *enhance* the sensor response to deformation. This paper focuses on the concept of such sensors and introduces the physics of an electrostriction enhanced sensing approach. We present experimental comparison with a solid-state capacitor with traditional air-gap capacitor elements.

In Section II, we consider deformation of a parallel-plate capacitor with a weakly polarizable gas (e.g., air) or vacuum between the electrodes. Such systems have traditionally been employed in sensor applications and analyzed by many researchers (see, for example, [14] and references within). Pressure or stress transmitted to the capacitor electrodes deforms them and alters the capacitance of the sensing element. The response of such a system is defined by elastic properties of electrodes (i.e. membranes), which makes the system very sensitive to overloads, e.g., large forces can damage the membrane or cause the electronics to short. In some capacitance sensor devices, an intervening thin film of dielectric material is introduced to enable sensor operation in so called “touch mode” [1], [9], [13]. When the thickness of the dielectric layer in “touch mode” is comparable with the capacitance gap, deformation of the layer and its electrostriction properties *should* be taken into account (and such a device will resemble the system presented within this paper).

In Section III, we promote a solid-state capacitor as an alternative to a vacuum-gap sensor solution for pressure, stress/strain, and tactile sensing. A dielectric material between electrodes increases the capacitance of the capacitor proportional to the material’s dielectric constant,  $\epsilon$ . However, the effect of deformation on the dielectric constant has not been sufficiently explored in the literature. Thus, in Section III-A, we discuss the underlying physics, presently available models and experiments on the effect of deformation on the dielectric constant. In our analysis, we deliberately do not limit the choice

Manuscript received August 24, 2000; revised January 21, 2003 and February 6, 2003. This work was supported by the University of Wisconsin Vilas Foundation.

The authors are with the Department of Mechanical Engineering at the University of Wisconsin-Madison, Madison, WI 53705 USA.

Digital Object Identifier 10.1109/TMECH.2003.816805

of materials embedded between the sensor electrodes—any existing elastic dielectric material can be used. For example, a part of a manipulator, transducer, or construction element can be used as a part of the sensor avoiding excessive “interface layers” between the material and the sensing mechanism. In Section III-B, we describe an experimental setup and instrumentation designed for simultaneous study of the performance under similar loads for both vacuum-gap and solid-state capacitance systems. The solid-state capacitor is a more robust system than air-gap capacitors. Application of large stress elicits a nonlinear response without collapsing the sensor, which is demonstrated in Section III-C by successful operation of the sensing element with bias loads varying by six orders of magnitude. In addition, electrostriction enhancement of solid-state capacitance sensors produce a higher response signal. Such sensors are easier to manufacture, and allow variable geometry (can bend, mold, twist, etc) than their vacuum-gap counterparts. There is a great variety of materials for optimization dynamic properties and environmental requirements of solid-state capacitor elements: although not addressed in this paper, future investigations may determine the engineering materials tailored for specific sensor applications.

In Section IV, we summarize the results obtained for the solid-state system in previous sections, formulate limitations and possible further development of polymer based sensors.

## II. DEFORMATION OF AIR-GAP CAPACITORS

Capacitance is defined as the ratio of an electric charge on a conductor and an electric potential induced by the charge. Because the electrostatic equations in vacuum are linear and homogeneous, relations between charges and potentials are linear and, thus, the capacitance of any system of conductors is typically modeled by their geometry alone (for simple geometries). Sensor applications rely on precise measurements of the effect of electrode deformation or displacement on the capacitance of the system. Special care should be taken to control any conductors in the surrounding sensor space, which could also affect capacitance measurements.

A basic design element in many sensor and transducer applications is a parallel-plate capacitor with a vacuum between the electrodes which is the simplest possible configuration whose performance is not affected by surrounding conductors and that can be easily analyzed. This design is typical for most micro-machined capacitance sensors and for microscopic pressure and tactile capacitor sensors [14]. A capacitor filled with gas (e.g., air) between the electrodes has similar properties as a vacuum-filled capacitor if the gas is able to escape during the motion of the electrode plates. Such systems will, henceforth, be referred to as “air-gap” capacitors. Capacitance response of devices with the gas sealed inside (i.e., compressed if the electrodes are moving) depends on the electrostriction properties of the gas, which is further discussed in Section III. The capacitance,  $C$ , of a parallel-plate capacitor with an area,  $A$ , and a gap,  $h \ll \sqrt{A}$ , between the plates is [16]

$$C = \frac{\epsilon\epsilon_0 A}{h} \left[ 1 + O\left(\frac{\log\left(\frac{\sqrt{A}}{h}\right)}{\frac{2\sqrt{A}}{h}}\right) \right] \quad (1)$$

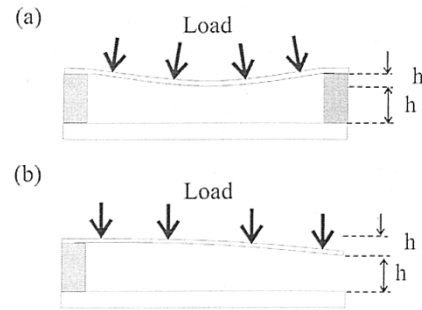


Fig. 1. Capacitance of the system varies due to deformation of the flexible electrodes. The system depends on the elastic properties of the electrodes. Overload can damage electrodes or short the electronics.

where  $\epsilon$  is the dielectric constant of the material between the plates (for air is  $\epsilon \approx 1$ ), and  $\epsilon_0 \approx 8.85 \times 10^{-12}$  F/m is the dielectric permittivity of free space. The contribution of a fringe effect estimated by the second term in the brackets and, for the capacitors geometry reported in the experimental part of this paper, is less than 1% of the total capacitance and will be ignored in the following analysis.

Consider the magnitude of capacitor output typical for sensor applications. For a 1-cm<sup>2</sup> plate with a 100- $\mu$ m air gap, the capacitance is 8.85 pF, an equivalent capacitance can be achieved with a 1-mm<sup>2</sup> plate with a 1- $\mu$ m air gap. One can see that it is not practical to make an air-gap sensor with capacitance larger than 100 pF, from the other hand, it is difficult to work with a sensor whose capacitance is less than 1 pF, unless one incorporates sophisticated “on-board” signal conditioning electronics [26]. Thus, for a stand-alone sensors, the expected range of capacitance is 1–100 pF.

The change in capacitance due to deformation or displacement of the electrodes can be registered by a variety of well-established methods (see, e.g., [14, p. 219]). However, precision fabrication is required to produce electrodes very close and highly parallel to one another, limiting capacitance sensing to situations in which the expense associated with the sensor fabrication is acceptable. Fig. 1 presents design ideas for air-gap sensors with flexible electrodes. Such systems have simple construction and high sensitivity, but their response is nonlinear and is defined by the elastic properties of the electrodes (membrane). While more rugged than piezoresistive pressure sensors, capacitive air-gap devices are sensitive to overloads. While some over-range protection is provided by the fixed electrode, excessive forces can damage the membrane or cause the electronics to short. The device presented here further improves upon the inherent over-range protection provided by the fixed electrode.

The dynamic response on deformation of a parallel-plate capacitor with rigid electrodes is defined by the elastic properties of the spacers keeping the electrode plates apart [Fig. 2(a)]. The problems of overload and shorting seen in a flexible electrode designs are less important here because the electrodes can be made sufficiently thick to withstand any expected loads. Performance and linear response of this system are simple to analyze—the relationship between the displacement and change in capacitance is approximately linear for small variations in the separation. The relative change in capacitance caused by varia-

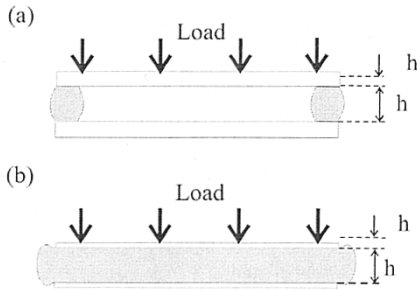


Fig. 2. Capacitor sensor designs with parallel displacements of plates. (a) Dynamic response of an air-gap parallel-plate capacitor with rigid electrodes is determined by elastic properties of the spacers keeping the electrode plates apart. (b) Dynamic response of the solid-state sensor under deformation depends on the elastic properties of the dielectric material between the electrodes.

tion in the gap thickness  $h$  between rigid electrodes is given by [14]

$$\frac{\Delta C}{C} = -\frac{\Delta h}{h}. \quad (2)$$

This expression implements two assumptions. First, it is assumed that the dielectric constant does not change, which is only valid if the fluid dielectric can “escape” during deformation. Second, the electrodes are not deformed, hence a term of the form  $\Delta A/A$  is absent. Equation (2) is quite accurate—indeed, for a large number of sensor applications where deformations are in the range of 10%, the terms omitted in (2) are of the order of 1%, which is less than the nonlinearity in the elastic response of most solid materials under similar deformations. However, in manufacturing of air-gap capacitors with rigid electrodes and elastic spacers it is difficult to ensure parallel placement (although advances in micromachining facilitate this process). In the following sections we discuss solid-state sensors having parallel-plate design and similar operational principles as considered above, but which have fewer construction/robustness problems than the air-gap capacitors.

### III. SOLID-STATE CAPACITANCE SENSOR

An isotropic dielectric material of thickness,  $h$ , sandwiched between two electrodes [Fig. 2(b)] composes a parallel-plate solid-state capacitor. A solid-state capacitor is simple to construct with multiple choices for materials and technologies for forming uniformly thin dielectric layers. This design ensures robustness of the sensor because the mechanical properties of the electrodes are not so important. High overload deformations elicit only a nonlinear response without collapsing the sensor, and the sensor geometry can vary with bending, twisting, etc. In contrast, the mechanical properties of the electrodes in the air-gap design will determine the degree of bending and twisting, which, under high overload conditions, will damage the sensor. For many applications, it can be very helpful to embed a sensor within existing material making the sensor a part of the device itself. For example, in many tactile-sensing applications (see, e.g., [2]) multiple layers are used including foam layers to add compliance, external surface materials for adding friction, and internal layers for sensing. The solid-state capacitor can be constructed as part of an existing layer avoiding

additional layers. The dielectric material between electrodes increases the total capacitance of the sensor which reduces the effects of parasitic capacitances. Furthermore, the dielectric material between electrodes increases the sensor response (see Section III-A and Table I) proportionally to the dielectric constant,  $\epsilon$ , thus simplifying the processing/conditioning of sensed signals. The dynamic response of the solid-state sensor under deformation depends on the elastic properties of the dielectric material between the electrodes—its Young’s modulus  $E_y$  and Poisson’s ratio  $\nu$ .

The same material parameters responsible for the deformation effect on the dielectric properties of the material define an electric-field-induced stress in the material. This phenomenon is called *electrostriction* [16], [25]. Similarly, a contribution of the effect of deformation on the dielectric constant is called *electrostriction enhancement* of the sensor response. This effect has not been sufficiently explored in the current literature on sensors, which limits application of all the benefits of the solid-state design approach in real devices. The goal of this paper is to present the available results on electrostriction of linear dielectrics and to experimentally demonstrate that dielectric material *amplifies* the capacitance response on deformation.

#### A. Theoretical Analysis

A capacitance change of a solid-state capacitor due to normal displacement of the plates can be obtained by considering a variation of (1). A relative capacitance change  $\Delta C/C$  is composed of three terms—a relative variation of the gap thickness  $-\Delta h/h$ , a variation of the electrode area  $\Delta A/A$ , and a variation of the dielectric constant  $\Delta\epsilon/\epsilon$  under the deformation

$$\frac{\Delta C}{C} = -\frac{\Delta h}{h} + \frac{\Delta A}{A} + \frac{\Delta\epsilon}{\epsilon}. \quad (3)$$

Notice that (3) contains two additional terms,  $\Delta A/A$  and  $\Delta\epsilon/\epsilon$ , which were absent in a similar relation for the air-gap system (2). We include the term  $\Delta A/A$  here because the electrodes can be deformable. The relationship between the terms  $-\Delta h/h$  and  $\Delta A/A$  follows from the solution of a boundary value problem of the elastic deformation and can be summarized as  $\Delta A/A = -k_A \Delta h/h$ , where the coefficient  $0 \leq k_A \leq 1$  depends on boundary conditions on the dielectric–electrode interface and elastic properties of both the dielectric and the electrodes. Two limit values of  $k_A$  can be obtained right away: the area of rigid undeformable electrodes is a constant, which corresponds to  $k_A = 0$ , and a variation of volume of an incompressible dielectrics in the gap between thin-film electrodes ( $\Delta V/V = \Delta h/h + \Delta A/A = 0$ , because  $\Delta V = 0$ ) leads to  $k_A = 1$ . An intermediate value of  $k_A$  can be obtained by consideration of deformations of a multilayer dielectric electrode system.

*Sensor Response Defined by  $\Delta\epsilon/\epsilon$ :* This section outlines results on the deformation effect on the dielectric constant  $\epsilon$  accounted for by the term  $\Delta\epsilon/\epsilon$  in (3). This term is absent only for capacitors where the liquid or gaseous dielectric can leak out during displacement of the electrode plates. The following is a demonstration that the term  $\Delta\epsilon/\epsilon$  constitutes a *major* contribution to the total sensor response on deformations that cannot be neglected.

TABLE I

SUMMARY TABLE FOR  $\Delta C/C = -k_\alpha \Delta h/h$ , WHERE  $k_\alpha$  IS CALCULATED FOR CONSTRAINED/UNCONSTRAINED FILM, RIGID/FLEXIBLE ELECTRODES

constrained	non - constrained/rigid electrodes	non - constrained/thin electrodes
$k_\alpha = \frac{(\epsilon-1)(\epsilon+2)}{3\epsilon} + \frac{4(\epsilon-1)^2}{15\epsilon} + 1$	$k_\alpha = \frac{(\epsilon-1)(\epsilon+2)}{3\epsilon} - \frac{2(\epsilon-1)^2}{15\epsilon} + 1$	$k_\alpha = \frac{(\epsilon-1)(\epsilon+2)}{3\epsilon} - \frac{2(\epsilon-1)^2}{15\epsilon} + 2$

An initially isotropic dielectric material becomes anisotropic after deformation and should be described by a second rank dielectric tensor,  $\epsilon_{ik}$ . The dielectric tensor of the deformed material can be presented<sup>1</sup> as [16], [25]

$$\epsilon_{ik} = \epsilon \delta_{ik} + \alpha_1 u_{ik} + \alpha_2 u_{kk} \delta_{ik} \quad (4)$$

which is a general linear functional relation between two second rank tensors  $\epsilon_{ik}$  and  $u_{ik}$ . In this expression  $\epsilon$  is the relative dielectric constant of the undeformed material,  $\delta_{ik}$  is the unit tensor,  $\alpha_1$  and  $\alpha_2$  are electrostriction constants. Parameter  $\alpha_1$  describes an effect of shear deformation on the dielectric properties of the material, and  $\alpha_2$  describes an effect of volume deformation on the dielectric properties of the material. For small displacements, the strain tensor,  $u_{ik}$  has the form  $u_{ik} = (1/2)(\partial u_i/\partial x_k + \partial u_k/\partial x_i)$ , where  $\mathbf{u} = (u_1, u_2, u_3)$  is the deformation displacement field, and  $\mathbf{x} = (x_1, x_2, x_3)$  are local coordinates. The sum  $u_{kk} = u_{11} + u_{22} + u_{33} \approx \Delta V/V$  represents a relative change in volume of the deformed material. Note, that the deformation effect on dielectric properties is an exact analog of the well-known photomechanical effect (change in refractive index in transparent materials with deformation) observed in the optical range of the electromagnetic spectrum. Fig. 3 illustrates a deformation effect on a cubic system of polarizable inclusions dispersed in an elastic media. The inclusion model accurately presents a composite of mesoscopic particles, but, with some limitations, can also be applied, to model molecules, ions or atoms of which a material is composed. Polarization of each inclusion depends on the local electrostatic field  $\mathbf{E}_{loc}$ , which is the sum of an applied field  $\mathbf{E}$ , and dipole fields  $\mathbf{p}$ , over all other inclusions. Distribution of polarizable inclusions, and, therefore, their contribution to the local field can be affected by deformation causing an induced anisotropy of dielectric properties of the material.

Let us orient a Cartesian coordinate system such that the plates of the capacitor are in the  $\mathbf{e}_1 \times \mathbf{e}_2$  plane, and the plate displacement occurs in the  $\mathbf{e}_3$  direction. A relative change of the gap  $\Delta h$  corresponds to the strain tensor components of the deformed elastic dielectric  $u_{33} = \Delta h/h$ . The relative volume change  $u_{kk}$  is  $u_{kk} = u_{33}$  and  $u_{kk} = 0$  for constrained and unconstrained incompressible materials, respectively. Capacitance measurements reveal a  $\epsilon_{33}$  component of the dielectric tensor, which determines a variation,  $\Delta \epsilon = \epsilon_{33} - \epsilon$ , contribution to the deformation response of the sensor. We have

$$\Delta \epsilon = (\alpha_1 + k_\epsilon \alpha_2) \frac{\Delta h}{h}, \quad 0 \leq k_\epsilon \leq 1 \quad (5)$$

where  $k_\epsilon = 0$  for unconstrained incompressible dielectric, and  $k_\epsilon = 1$  for constrained material. The parameters  $\alpha_1$  and  $\alpha_2$ , first introduced in [16], [25], define an electric-field-induced stress

<sup>1</sup>Using summation notation.

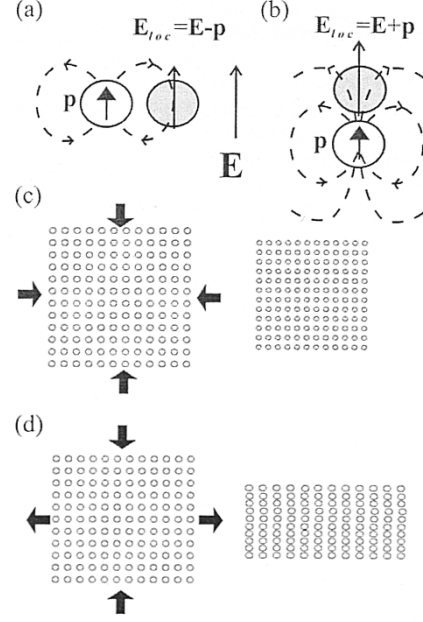


Fig. 3. Cubic structure of polarizable inclusions as an illustration of the deformation effect on polarization. Polarization of each inclusion depends on a local electrostatic field,  $\mathbf{E}_{loc}$ , which is the sum of an applied field  $\mathbf{E}$ , and of dipole fields  $\mathbf{p}$  of all other inclusions. A contribution to the local field depends on relative position of inclusions. (a) Parallel placement of inclusions reduces the local field. (b) Inclusions lined up with each other increases the local field. (c) Volume compression, increases the inclusion density, which is described by parameter  $\alpha_2$ . (d) Pure shear deformation moves the inclusions closer in one direction and separates them further apart in another direction, which creates an anisotropy of dielectric properties described by parameter  $\alpha_1$ .

in dielectric materials and are called “electrostriction parameters.” For polarizable fluids these parameters are estimated in [25] as

$$\alpha_1 = 0 \quad \text{and} \quad \alpha_2 = -\frac{(\epsilon-1)(\epsilon+2)}{3}. \quad (6)$$

A similar theoretical model for elastic solids from [23] predicts electrostriction parameters as

$$\alpha_1 = -\frac{2}{5}(\epsilon-1)^2 \quad \text{and} \quad \alpha_2 = -\frac{(\epsilon-1)(\epsilon+2)}{3} + \frac{2}{15}(\epsilon-1)^2. \quad (7)$$

Theoretical estimates of the relation between  $\Delta \epsilon/\epsilon$  and  $\Delta h/h$  obtained from (5) and (7) for  $k_\epsilon = 0$  and 1 are plotted in Fig. 4. This plot also presents experimental measurement of the coefficient  $(\alpha_1 + k_\epsilon \alpha_2)$  obtained for several dielectric materials combined with data from [23]. One can see that the theoretical predictions for constrained materials ( $k_\epsilon = 1$ ) agree with experimental data.

The relationship between the variation of the sensor capacitance and deformation  $\Delta h/h$  can be summarized as

$$\frac{\Delta C}{C} = -k_\alpha \frac{\Delta h}{h}.$$

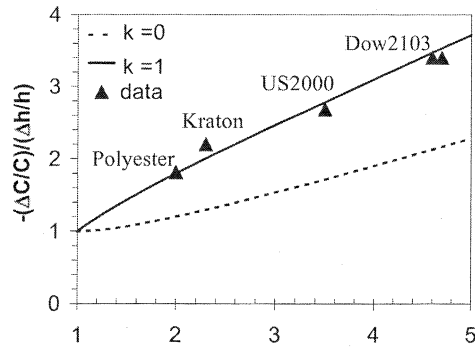


Fig. 4. This plot presents relationships between  $\Delta\epsilon/\epsilon$  and  $-\Delta h/h (= k_\alpha)$  for  $k_\epsilon = 0$  (incompressible dielectric) and  $k_\epsilon = 1$  (constrained to the electrodes dielectric). Triangles represent measured values for Polyester "D," Dow-2103-80AE, and values for Kraton, Dow-2103-80AE, and US2000 obtained from [23]. One can see  $k_\alpha > 1$  for all dielectric materials confirming that the dielectric between the electrodes enhances the sensor deformation response due to electrostriction effects.

Values for  $k_\alpha$  are presented in Table I. Notice that these terms are trivial when  $\epsilon = 1$ . For other values of  $\epsilon$ ,  $k_\alpha > 1$ , which indicates that a dielectric material *amplifies* the sensor response.

1) *Load Stress—Deformation Relations*: The deformation registered by the sensor is determined by elastic properties of the dielectric material and the mechanical conditions on its surface. We distinguish several typical boundary conditions in the stress analysis.

- 1) Elastic properties of electrodes do not affect deformation of the dielectric layer, which is correct for thin, easily deformable electrodes, or for rigid electrodes with the frictionless slipping dielectric layer. The elastic response from normal stress of both systems is similar; thus, we will refer to this situation as a *nonconstrained elastic dielectric*.
- 2) Only a normal deformation is allowed for rigid electrodes attached to the dielectric. We will refer to such a configuration as a *constrained elastic dielectric*.
- 3) Intermediate configuration where both elastic properties of the electrodes and interface layer between the dielectric and the electrodes contribute to an elastic response of the sensor. Analysis of such a configuration is beyond the scope of the present paper, but can be provided for a particular system.

Let us consider compression of the sensor under some normal stress  $\sigma_{nn} = F_n/A$  where  $F_n$  is the force applied over area  $A$ . We choose a coordinate system such that the normal stress is  $\sigma_{nn} \equiv \sigma_{33}$ . Resulting from this stress deformation  $u_{33}$  is determined by Young's modulus,  $E_y$ , and Poisson's ratio,  $\nu$  of the dielectric. For normal deformation of a parallel-plate capacitor  $u_{33} = \Delta h/h$ , the strain/stress relation for a *nonconstrained dielectric material* is [15]

$$\frac{\Delta h}{h} = -\frac{\sigma_{nn}}{E_y} \quad (8)$$

and for a *constrained dielectric material*

$$\frac{\Delta h}{h} = -\frac{(1+\nu)(1-2\nu)}{(1-\nu)} \frac{\sigma_{nn}}{E_y} \quad (9)$$

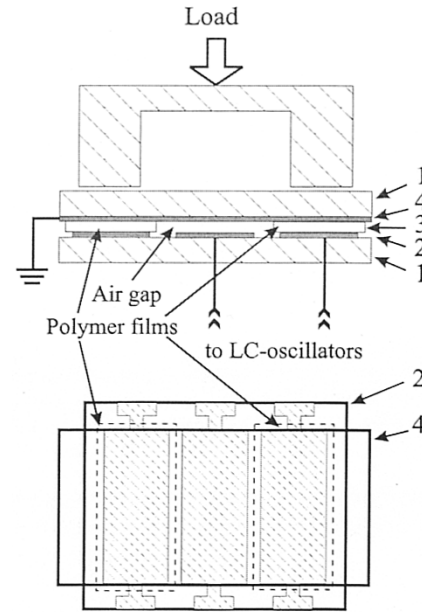


Fig. 5. Schematic diagram of the polymer-air-polymer capacitor assembly (not to scale). The different layers are: 1—glass slides; 2—three-electrode system; 3—polymer films and air gap; and 4—ground electrode. Weight load on the top of the  $\Pi$ -shaped frame deforms the polymer film. The change in capacitance across the polymer and the air capacitors are registered by LC oscillators.

Note that the elastic response of constrained dielectric material depends on Poisson's ratio  $\nu$ , which, for most solid materials, is in the range  $\nu = 0.2-0.4$ , but for many polymers it is very close to the value for incompressible materials, 0.5 (e.g.,  $\nu = 0.45-0.499$ ) [6]. Thus, Poisson's ratio is important for the deformation of constrained systems and should be taken into account in particular designs.

### B. Experimental Setup

We compare a polymer-film solid-state capacitor and an air-gap capacitor of similar geometry by studying a composite polymer-air-polymer system under an applied load. The capacitors are formed by two glass plates with vapor deposited electrodes (Fig. 5). One glass plate is patterned with three separated electrodes, each  $0.75 \times 2.0 \text{ in}^2$ , and the second glass plate carries a large grounded electrode. Two pieces of the same polymer film are placed between each of the outer electrodes and the ground electrode. These two polymer films, which constitute a single polymer-film capacitor, act as a spacer for the center air-gap capacitor. Experiments are conducted by applying a load to the glass plate carrying the ground electrode, and measuring the capacitance change independently for the polymer-film and for the air-gap capacitors. The presence of the load produces a small capacitance change for both the air-gap capacitor and the polymer film capacitor. For the air-gap capacitor, the change arising from only the change in the gap is given by (2). For the polymer-film capacitor, the capacitance change contains contributions from the gap change as well as the permittivity change, and is given by (3), where  $\Delta A/A \equiv 0$ . The gap change for both capacitors is the same.

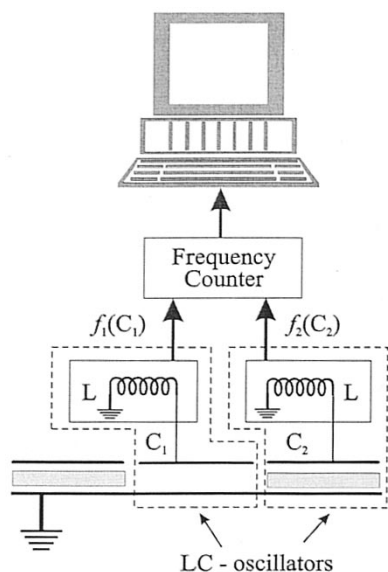


Fig. 6. Schematic diagram of the measurement apparatus. The system measures the change in oscillator frequency due to a capacitance change arising from the film deformation. Two independent  $LC$  oscillators with equal inductances,  $L$ , formed by an air-gap capacitor,  $C_1$ , and a polymer-film capacitor,  $C_2$ , produce oscillations frequencies  $f_1$  and  $f_2$ , respectively. Movement of the glass plate with the ground electrode shifts oscillation frequencies which are measured by a two-channel frequency-counter data-acquisition board and recorded by a computer.

A schematic diagram of the measurement apparatus is presented in Fig. 6. Capacitance changes were determined by measuring the frequency change of a Hartley ( $LC$ ) oscillator circuit which included the sample capacitor. A similar setup to study polymer electrostriction has been discussed in [22]. The oscillation frequency,  $f$ , depends on the inductance,  $L$ , and capacitance,  $C$ , of the circuit. Because the inductance is independent of deformation and is constant during the test, a variation of the frequency is a result of variation in the capacitance  $C$ , which is related to the frequency change  $\Delta f$  by

$$\frac{\Delta C}{C^0} = -\beta \frac{\Delta f}{f^0} \quad (10)$$

where the superscript "0" refers to the reference state from which changes were measured. The coefficient  $\beta$  ( $\approx 3$ ) depends on the Hartley oscillator and the sample capacitance relative to the equivalent capacitance: this parameter is constant during measurements and determined by calibration. Frequency changes were measured with a Keithley PCIP-CNTR Counter/Timer. Values of the air-gap capacitors measured by General Radio  $RLC$  1689 Digibridge are in the range 30–50 pF, values for the polymer-gap capacitors were in range 50–190 pF, resulting in an  $LC$ -oscillator frequency in the range 0.7–1.2 MHz. Similar systems for measuring capacitance are described in [3], [8].

### C. Experimental Procedure and Results

Two commercially available polymer films were tested in this study, both with thickness of 0.004 in ( $10^{-4}$ m). The first sample is Dow 2103-80AE urethane-ether block copolymer, and

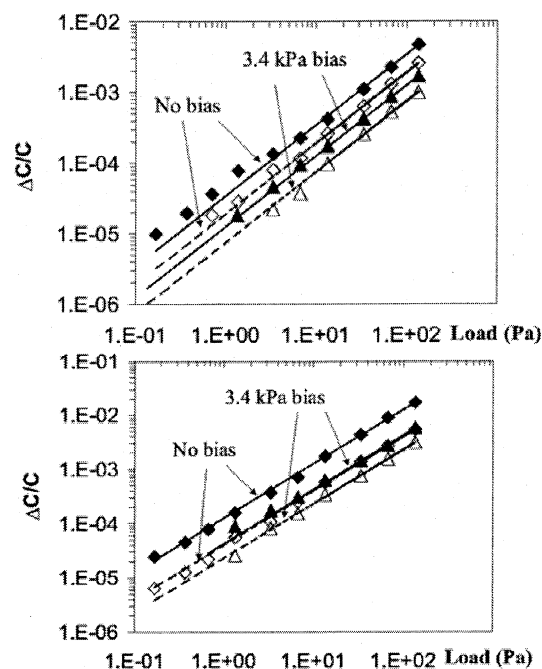


Fig. 7. Experimental data comparing air-gap and polymer-gap-capacitance sensor responses. Measurements for (a) polyester "D" and (b) urethane-ether Dow 2103-80AE polymer films are plotted on both log-log and linear axes. Data for the air-gap capacitor are shown by open symbols ( $\Delta$ ,  $\circ$ ). Data for the polymer-film capacitor are shown by closed symbols ( $\bullet$ ).

the second sample is Polyester "D" polymer film obtained from Transilwrap Company, Inc. We tested the sensitivity to deformation using bias weights of 50–2000 g giving bias stresses of 0.35–14 kPa, and variable weights added to the bias weights of 0.005–20 g resulting in load stresses of  $3.5 \times 10^{-2}$ –140 Pa. Results are discussed below.

The capacitance variation,  $\Delta C/C$ , caused by the deformation of the polymer films is presented as a function of applied mechanical stress in Figs. 7 and 8. The capacitance variations were determined from the change in oscillators frequencies, as described above, immediately after the stress was applied, using the state immediately preceding the stress as the reference.

Weight loads were applied manually using a  $\Pi$ -shaped frame on top of the glass plate of the three-electrode system (Fig. 5) to insure that the load stress was applied right across a polymer film on the outer electrodes. We believe that there was no bending of the glass plates and that the capacitance response of the system under the load is due to deformation of the polymer film alone. A variation of the air-gap is assumed to equal the deformation of the film between the electrodes.

Fig. 7 compares the response of an air-gap and polymer gap capacitance sensor. Both systems exhibit near linear response over the entire load range ( $3.5 \times 10^{-2}$ –140 Pa) measured across an air-gap and a polymer-gap capacitors. Good sensitivity to deformation was achieved over the entire range of bias stresses (0.35–14 kPa). As an example we present measurements for 0 Pa and 3.4-kPa load biases. Data for the 3.4-kPa bias produces lower, but still easily measurable response when compared with film with no extra load bias.

Relative variations of capacitance obtained for the air-gap capacitor (open symbols in the plots),  $\Delta C_{\text{air}}$ , have opposite sign

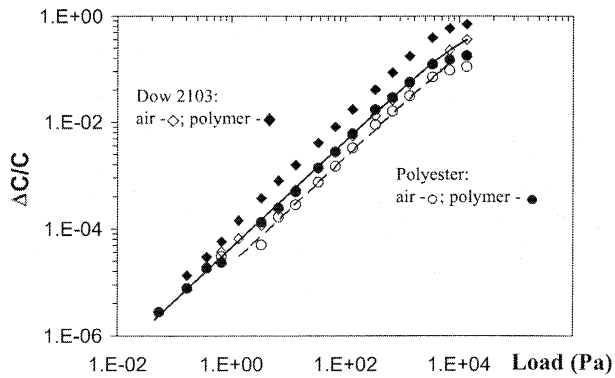


Fig. 8. Comparison of air-gap and polymer gap capacitance sensor responses for loads over six orders of magnitude. Sensitivity to small deformation is defined by the slope of the data which is linear except for large biases. The same effect can also be seen in Fig. 7. Solid (urethane) and dashed (polyester) lines represent theoretical predictions of an effective elastic modulus of rubber-like materials [18].

and are equal to relative variations of the capacitor-gap magnitude ( $\Delta C_{\text{air}}/C_{\text{air}} = -\Delta h/h$ ). Variations of the polymer-film capacitor (solid symbols on the plots),  $\Delta C_{\text{pol}}$ , have larger magnitude than variations of the air-gap capacitor, which is in agreement with the theoretical analysis in Section III-A ( $\Delta C_{\text{pol}}/C_{\text{pol}} = -k_{\alpha}\Delta h/h$ ,  $k_{\alpha} > 1$ ). The polyurethane film (Dow 2103-80AE) is softer than the polyester film and, thus, has larger air-gap capacitance response. Electrostriction enhancement of a solid sensor with polyester is 1.8 and with urethane polymer is 3.5. The dielectric constant of the polyurethane polymer ( $\epsilon = 4.6$ ) is higher than the constant of the polyester polymer ( $\epsilon = 2$ ), which explains the greater *electrostriction enhancement* of the polyurethane-film capacitor response under deformation [and dielectric materials with higher dielectric constants will further enhance the sensor sensitivity in accordance with (7)]. Because both air-gap and the polymer-film capacitors have the same area and gap thickness, dielectric constants of both polymers are obtained as a ratio of absolute capacitance values of polymer-film and air-gap capacitors (see (1)).

The coefficient  $k_{\alpha}$  is determined as ratio of slopes of stress dependence of  $\Delta C_{\text{pol}}/C_{\text{pol}}$  and  $\Delta C_{\text{air}}/C_{\text{air}}$  in Fig. 7. Experimental values of coefficient  $k_{\alpha}$  obtained for both polymers are given in the plots in Fig. 4 and are in good agreement with theoretical predictions for constrained dielectric films. Note, that a prediction of coefficient  $k_{\alpha}$  by (7) is derived for isotropic solids and is not valid for polymer films under bias loads which create a compression induced anisotropy of dielectric properties of films.

Fig. 8 demonstrates a capacitance response of both polymer films in six order of magnitude range of the loads. The sensitivity of capacitance measurements to small stress under an arbitrary bias load is defined by the slope at a corresponding point in the plot of Fig. 8 for either air-gap or polymer-film capacitance measurements. The sensitivity to small deformation becomes smaller as the bias loads increase. The same effect can be seen by comparing slopes for loaded and unloaded films on the plots in Fig. 7. Even for the maximum bias applied, the solid-state capacitor demonstrated good sensitivity to small deformations.

#### IV. DISCUSSION AND CONCLUSION

In this paper, we analyzed a solid-state capacitor for applications in stress/strain, pressure, and tactile sensing. The solid-state sensor is more robust than a vacuum-gap capacitor—application of large overload stress elicits a nonlinear response without collapsing the sensor. Solid-state sensors are easier to manufacture, with selection of variety of materials potentially optimized by dynamic properties, environmental requirements, etc. Such a sensor can be embedded within existing materials of a device and, thus, avoid excessive “interface layers.” In this paper, we showed an experimental setup for simultaneous studying performance of air-gap and solid-state capacitance sensors. We presented data to compare the performance under stress-induced deformation of solid-state and air-gap capacitors with two different commercially available polymeric materials between the electrodes. These preliminary data show a high deformation sensitivity of polymer-based solid-state sensors under a wide range of mechanical loads.

Applications of solid-state capacitor sensors for tactile sensing requires sensors with sizes of 2–4 mm<sup>2</sup>, smaller sizes may be desirable for other sensor solutions. Scaling down of the area and the gap thickness of the system analyzed in this paper is possible while maintaining the equivalent total capacitances. Incorporating more sophisticated signal processing than was used in the experimental part of this work will allow further reduction of sensor sizes and improvement of the sensitivity. Future studies aimed at constructing arrays of microscaled solid-state capacitance sensors for use in tactile sensing are currently underway (see, e.g., [7]).

The theoretical analysis was developed for isotropic linear elastic and linear dielectric materials. These assumptions are not exactly valid for polymeric materials, whose mechanical response is viscoelastic and whose electric behavior can be quite different from a linear dielectric model. At present, there are no models available for electrostriction constants of polymeric materials, but as presented in this paper linear elastic and dielectric analysis is still in good agreement with the polymer response under moderate bias loads. It should be noted that some polymer films are electrically and mechanically anisotropic due to axial or bi-axial stretching or forming surface layers during processing. Thus, tension modulus reported for a plane extension of the material can be different from the values obtained for normal deformations. Some very interesting sensing ideas can come from employing uniaxially anisotropic materials in solid-state sensors. Electrostriction response of anisotropic materials is different from the analysis reported in this paper. Such materials can have larger electrostriction response than isotropic materials and can be sensitive to shear deformations even with a parallel-plate capacitor setup [24].

An electrostriction enhanced sensor has dielectric material between the electrodes. It is known that environmental conditions such as humidity, temperature and chemical vapor may affect dielectric properties of the polymer and cause cross-sensitivity. Electrostriction sensors are similar in this respect to resistive sensors (while piezoresistive sensors are less sensitive to humidity and chemical vapor effects). If a cross sensitivity is not desirable, then, special efforts should be made to isolate the

sensor from the environment, to select or develop materials with low sensitivity to such conditions. We are currently working on the design of materials which have weak sensitivity to temperature and humidity. For some applications such sensitivity is not important.

Polymer properties of the dielectric material may affect the long-term behavior of the sensor. While the polymer layer will perform well under cyclic loading, static loading will degrade performance due to viscoelastic flow of the material, however, the use of high frequency vibration to reduce these affects is under study [12].

Further study should be conducted on engineering materials tailored for specific sensor applications. New materials such as polymer composites of nano-size particles, metal-cluster block co-polymers, or ceramics with improved dielectric and elastic properties should be tested as possible candidates for sensing applications.

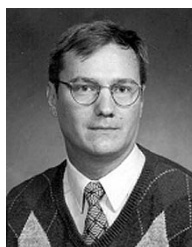
#### ACKNOWLEDGMENT

The authors wish to thank T. Osswald, S. Zauscher, and D. Klingenberg for helpful discussions.

#### REFERENCES

- [1] S. T. Cho, K. Najafi, C. L. Lowman, and K. D. Wise, "An ultrasensitive silicon pressure-based microflow sensor," *IEEE Electron. Devices*, vol. 39, pp. 825–835, Apr. 1992.
- [2] P. Dario and G. Buttazzo, "An anthropomorphic robot finger for investigating artificial tactile perception," *Int. J. Robot. Res.*, vol. 6, no. 3, pp. 25–48, 1987.
- [3] E. O. Doebelin, *Measurement Systems: Application and Design*, 4th ed. New York: McGraw-Hill, 1990.
- [4] R. S. Fearing, "Tactile sensing mechanisms," *Int. J. Robot. Res.*, vol. 9, no. 3, pp. 3–23, 1990.
- [5] N. J. Ferrier and R. W. Brockett, "Reconstruction of the shape of a deformable membrane from image data," *Int. J. Robot. Res.*, vol. 19, no. 9, pp. 795–816, 2000.
- [6] J. D. Ferry, *Viscoelastic Properties of Polymers*. New York: Wiley, 1980.
- [7] T. R. Filanc-Bowen, G. H. Kim, and Y. M. Shkel, "Novel sensor technology for shear and normal strain detection with generalized electrostriction," in *Proc. IEEE Conf. Sensors*. Orlando, FL, June 12–14, 2002.
- [8] S. Franco, *Design With Operational Amplifiers and Analog Integrated Circuits*. New York: McGraw-Hill, 1980.
- [9] M. Gad-el-Hak, Ed., *The MEMS Handbook*. Boca Raton, FL: CRC Press, 2002.
- [10] R. D. Howe, "Tactile sensing and control of robotic manipulation," *J. Adv. Robot.*, vol. 8, no. 3, pp. 245–261, 1994.
- [11] D. Hristu, N. J. Ferrier, and R. W. Brockett, "The performance of a deformable-membrane tactile sensor: Basic results on geometrically-defined tasks," in *Proc. IEEE Int. Conf. Robotics Automation*, vol. 1, Apr. 2000, pp. 508–513.
- [12] G. H. Kim and Y. M. Shkel, "Sensing shear strains with electrostriction effect in solid electrorheological composites," *J. Intell. Mater. Syst., Stru.*, vol. 13, pp. 479–483, 2002.
- [13] W. H. Ko, Q. Wang, and Y. Wang, "touch mode pressure sensors for industrial Applications," in *Proc. Solid-State Sensor Actuator Workshop*, 1996, pp. 244–248.

- [14] G. Kovacs, *Micromachined Transducers: Sourcebook*. New York: MacGraw-Hill, 1998.
- [15] L. D. Landau and E. M. Lifshitz, *Theory of Elasticity*. London, U.K.: Butterworth-Heinemann, 1995.
- [16] —, *Electrodynamics of Continuous Media*. New York: Pergamon, 1984.
- [17] E. J. Nicolson and R. S. Fearing, "Sensing capabilities of linear elastic cylindrical fingers," in *Proc. RSJ/IEEE Int. Conf. Intelligent Robots Systems*, vol. 1, July 1993, pp. 178–185.
- [18] T. A. Osswald and G. Menges, *Materials Science of Polymers for Engineers*, 2nd ed. Munich, Germany: Hanser, 2003.
- [19] T-2000 TactArray Capacitive Sensor, Pressure Profile Systems (2003). [Online]. Available: <http://www.pressure-profile.com>
- [20] R. A. Russell, "Compliant-skin tactile sensor," in *Proc. IEEE Int. Conf. Robotics Automation*, vol. 4, June 1987, pp. 2221–2233.
- [21] A. A. Shimoga and K. B. Goldenberg, "Soft robotic fingertips part i: a comparison of construction materials," *Int. J. Robot. Res.*, vol. 15, no. 4, pp. 320–334, 1996.
- [22] Y. M. Shkel and D. J. Klingenberg, "Material parameters for electrostriction," *J. Appl. Phys.*, vol. 80, pp. 4566–4572, 1996.
- [23] —, "Electrostriction of polarizable materials. Comparison of models with experimental data," *J. Appl. Phys.*, vol. 83, no. 12, pp. 7834–7843, 1998.
- [24] —, "A continuum approach to electrorheology," *J. Rheol.*, vol. 45, no. 5, pp. 1307–1322, 1999.
- [25] J. A. Stratton, *Electromagnetic Theory*. New York: McGraw-Hill, 1941.
- [26] M. R. Wolfenbuttel and P. Regtien, "Design considerations for a silicon capacitive tactile sensor," *Sens. Actuators*, vol. 24A, no. 3, pp. 187–190, 1990.



**Yuri M. Shkel** (M'99–A'00) received the B.S. degree in mechanics and applied mathematics and the Ph.D. degree in fluid dynamics, from Moscow State University, Moscow, U.S.S.R., in 1984 and 1989, respectively.

Since 2000, he has been an Assistant Professor of Mechanical Engineering in the Department at University of Wisconsin, Madison. He holds an affiliate appointment in electrical and computer engineering at the same university. His research interests include electromagnetic field controllable

"smart" materials, sensor and actuator application of electrostriction and magnetostriction, nano-and micro-composite materials in electromagnetic field.



**Nicola J. Ferrier** (S'90–M'92) received the B.Sc. degree in applied mathematics and the M.Sc. degree in computing sciences from the University of Alberta, Edmonton, AB, Canada, and the S.M. and Ph.D. degrees in engineering and applied sciences from Harvard University, Cambridge, MA.

She is an Associate Professor in the Department of Mechanical Engineering at the University of Wisconsin-Madison. Her research interests are robotics and intelligent systems, focusing on the integration of visual and tactile sensors in robot control systems,

and concentrating primarily on active vision systems, attentive control, and dynamic tracking.